Available online at www.sciencedirect.com
ScienceDirect
Journal of Photochemistry and Photobiology A: Chemistry 184 (2006) 105–112
Journal of Photochemistry and Photobiology A:Chemistry
www.elsevier.com/locate/jphotochem

One- and two-photon photochemical stability of linear and branched fluorene derivatives

Claudia C. Corredor[a,b], Kevin D. Belfield[a,*], Mykhailo V. Bondar[c], Olga V. Przhonska[c], Sheng Yao[a]

[a] *Department of Chemistry and College of Optics and Photonics: CREOL and FPCE, University of Central Florida, P.O. Box 162366, Orlando, FL 32816-2366, USA*
[b] *Bristol-Myers Squibb Pharmaceutical Research Institute, One Squibb Drive, P.O. Box 191, New Brunswick, NJ 08903-0191, USA*
[c] *Institute of Physics, Prospect Nauki, 46, Kiev-28, 03028 Kiev, Ukraine*

Received 2 February 2006; accepted 29 March 2006
Available online 18 April 2006

Abstract

Photochemical decomposition of the fluorene derivatives, 4,4′-[[9,9-bis(ethyl)-9H-fluorene-2,7-diyl]di-2,1-ethenediyl]bis(*N*,*N*-diphenyl) benzeneamine (**1**) and 4,4′,4″-[[9,9-bis(ethyl)-9H-fluorene-2,4,7-triyl]tri-2,1-ethenediyl]tris(*N*,*N*-diphenyl)benzeneamine (**2**), were investigated in pTHF under one- (UV-lamp) and two-photon (femtosecond laser) excitation. The quantum yields of the photoreactions were determined by absorption and fluorescence methods in air-saturated and deoxygenated solutions. The values of quantum yields were in the range $(1.5–2.1) \times 10^{-6}$ for both types of irradiation, indicating that similar photobleaching processes occur under both one- and two-photon excitation. Deoxygenation of pTHF increased photostability of **1** and **2** by over an order of magnitude relative to air-saturated solutions. A cursory examination of some of the photochemical products (analyzed by HPLC and APCI-MS spectroscopy techniques) revealed an important role of ground state oxygen in the photoreactions, since no oxidation products were observed upon irradiation in the presence of the well know singlet oxygen sensitizer methylene blue.

Keywords: Photodecomposition; Two-photon absorption; Photobleaching; Fluorene photostability

1. Introduction

Fluorene derivatives with large two-photon absorption (2PA) cross-sections [1–3] exhibit desirable properties for the development of new non-linear optical technologies, particularly in the field of 3D microfabrication [4], optical power limiting [5], and two-photon fluorescence imaging [6]. Photodecomposition (the irreversible light-induced destruction of a material) is one of the main limitations of many organic dyes for their application in non-linear optics and photonics. Hence, the photochemical stability of organic dyes, such as fluorene derivatives, under one- and two-photon excitation is critical for a number of emerging non-linear optical applications. Photodecomposition of simple fluorene derivatives was investigated early on with regards to problems of environmental contamination [7,8]. Photolytic degradation of certain fluorene derivatives under UV irradiation and the dependence of photolysis kinetics on molecular weight and type of substituents were shown [9]. The effects of solvent and substituents on the photooxidation of a few fluorene derivatives and the photochemical behavior of fluorene at a silica gel/air interface have been investigated [10,11]. A theoretical study of the photo-oxidation of the 2PA chromophore AF50 [12] and formation of its possible photoproducts was reported [13].

Photochemical decomposition under two-photon excitation may well be different from the reactions induced by low intensity irradiation [14]. Even in the case when the same excited state of the molecule is populated under one- and two-photon excitation, additional photochemical processes, such as photoionization and bond fission [15], are possible for the latter type of excitation due to high irradiation intensities. There is evidence that in many dye systems, the photobleaching rates by two-photon excitation

* Corresponding author. Tel.: +1 407 823 1028.
E-mail address: kbelfiel@mail.ucf.edu (K.D. Belfield).

1010-6030/$ – see front matter © 2006 Elsevier B.V. All rights reserved.
doi:10.1016/j.jphotochem.2006.03.036

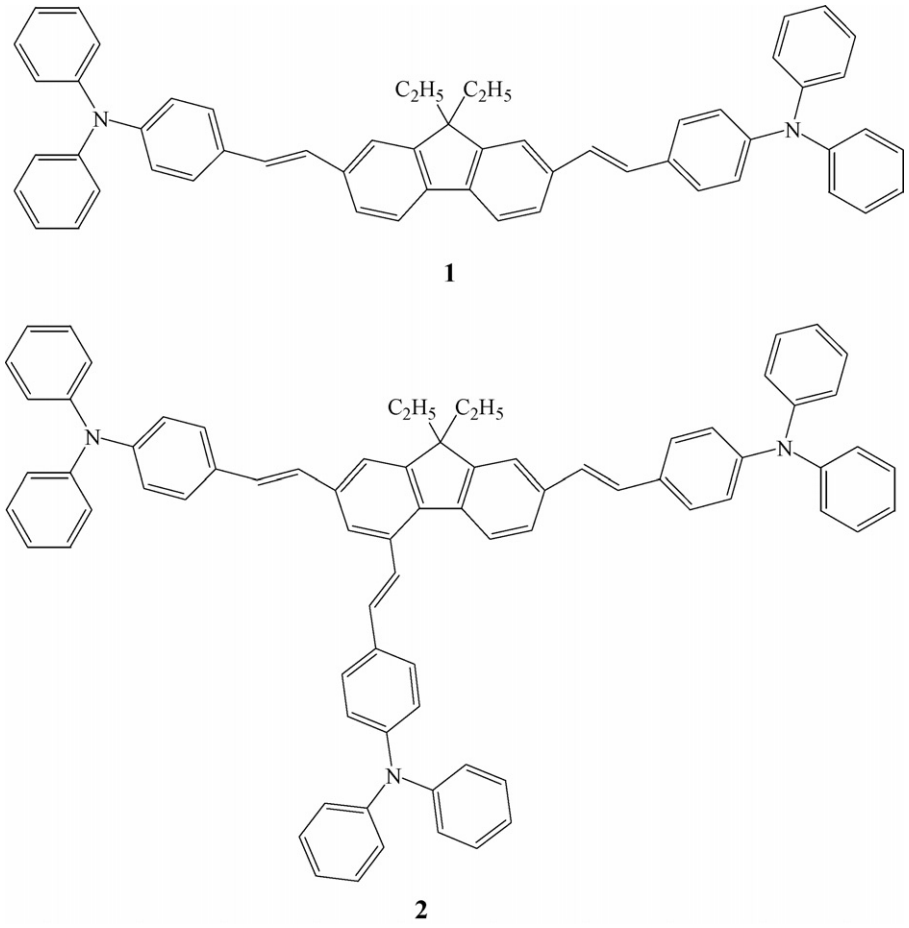

Fig. 1. Molecular structures of linear and branched fluorene derivatives **1** and **2**.

are significantly enhanced with respect to one-photon excitation at comparable photon-emission yields [16]. Until now, relatively little is known about two-photon photodecomposition of fluorene derivatives possessing high non-linear absorptivity. Preliminary investigation of photochemical processes of selected fluorene derivatives under two-photon excitation were investigated in our laboratory [17], and an increase in the photodecomposition quantum yield was observed for (7-benzothiazol-2-yl-9,9-didecylfluoren-2-yl)diphenylamine in CH_2Cl_2 under femtosecond two-photon excitation. The primary goal of this paper is the investigation of the photochemical stability of new linear and branched fluorene derivatives (Fig. 1) that possess large 2PA cross-sections (maximum values ~2000–4000 GM [18]). In addition, a cursory examination of several photoproducts of **1** and **2** was undertaken to provide some speculative, but informative, insight into the photodecomposition processes.

Potential photobleaching pathways were investigated by working at different dye concentration (to determine the dependence of photobleaching on concentration) and oxygen concentration. Oxygen, a strong triplet quencher, can minimize photobleaching via the triplet state, but on the other hand, reactive singlet oxygen (O_2 ($^1\Delta_g$)) can be generated by triplet–triplet annihilation between O_2 ($^3\Sigma_g^-$) and the dye molecule, both in their triplet states. Since some fluorene derivatives synthesized in our laboratory have the ability to generate singlet oxygen O_2 ($^1\Delta_g$) under single and two-photon excitation with high quantum yields ($\Phi_\Delta = 0.35$–0.75) [19,20], there is great interest in determining the effect of oxygen concentration on the photostability of these fluorenes derivatives. Photostability, or lack thereof, is often considered the Achilles Heel of organic photonic materials, and the studies reported herein are critical to determine the robustness and limitations of these potentially useful non-linear absorbing dyes.

2. Experimental

Photochemical properties of the fluorene derivatives 4,4′-[[9,9-bis(ethyl)-9H-fluorene-2,7-diyl]di-2,1-ethenediyl]bis(*N*,*N*-diphenyl)benzeneamine (**1**) and 4,4′,4″-[[9,9-bis(ethyl)-9H-fluorene-2,4,7-triyl]tri-2,1-ethenediyl]tris(*N*,*N*-diphenyl)benzeneamine (**2**) were studied in air-saturated and deoxygenated spectroscopic grade poly(tetrahydrofuran) (pTHF) (MW 250) at room temperature. The syntheses of **1** and **2** were described previously [21]. Deoxygenated solutions were obtained by bubbling Ar through the solutions for 30 min or repeated freeze–pump–thaw cycles (both procedures yielded identical results). The absorption spectra were recorded using an Agilent 8453 UV–visible spectrophotometer in 10 mm path length quartz cuvettes for concentrations, $C \leq 2 \times 10^{-5}$ M. The fluorescence, excitation, and excitation anisotropy spectra of **1** and

2 were obtained using a PTI Quantamaster spectrofluorimeter in 10 mm fluorometric quartz cuvettes for dilute solutions ($C \leq 10^{-6}$ M). Two-photon absorption cross-sections, σ_{2PA}, of **1** and **2** in pTHF were determined by an open aperture *Z*-scan method [22] and an up-converted fluorescence technique (relative to fluorescein in water) [23], using a femtosecond laser system (Clark-MXR, CPA2010, Ti:sapphire amplified system followed by an optical parametric generator/amplifier (TOPAS 4/800, Light Conversion) with pulse duration, $\tau_P \approx 140$ fs (FWHM), repetition rate, $f = 1$ kHz, tuning range 560–2100 nm and maximum average power, $P_0 \approx 25$ mW).

The quantum yields of the photochemical reactions of **1** and **2** in pTHF under one-photon and two-photon excitation were determined by absorption and fluorescence methods, described in detail in Refs. [17,20,24,25]. These methods are based on measurements of the temporal changes in the steady-state absorption and fluorescence spectra during irradiation, respectively. In the case of the absorption method, the quantum yields of the photochemical reactions under one-photon excitation, Φ_{1PA}, were determined by the equation [25]:

$$\Phi_{1PA} = \frac{[D(\lambda, 0) - D(\lambda, t_{ir})]N_A}{10^3 \varepsilon(\lambda) \int_\lambda \int_0^{t_{ir}} I_0(\lambda)[1 - 10^{-D(\lambda,t)}]\, d\lambda\, dt}, \quad (1)$$

where $D(\lambda, 0)$, $D(\lambda, t_{ir})$, $\varepsilon(\lambda)$, t and λ are the initial and final optical density of the solution, extinction coefficient ($M^{-1}\,cm^{-1}$), irradiation time (s) and excitation wavelength (cm), respectively; N_A the Avogadro's number; t_{ir} the total irradiation time; $I_0(\lambda)$ is the spectral distribution of the excitation irradiance.

The values of Φ_{1PA} were obtained also by employing a fluorescence method with corresponding equation [25]:

$$\Phi_{1PA} = \frac{1 - F(t_{ir})/F(0)}{\int_\lambda \int_0^{t_{ir}} I_0(\lambda)\sigma(\lambda)[F(t)/F(0)]\, d\lambda\, dt}, \quad (2)$$

where $F(0)$ and $F(t_{ir})$ are the initial and final fluorescence intensity expressed in relative arbitrary units (typically, in counts/s) and $\sigma(\lambda)$ is the one-photon absorption cross-section (cm^2). The experimental setup for one-photon excitation is shown in Fig. 2a. The entire volume of the fluorene solutions were irradiated simultaneously with the UV-lamp, LOCTITE 97034 (average irradiance, $I_0 \approx 130$ mW/cm^2), in the spectral range 400–440 nm (using glass UV–visible filters). In the case of the absorption method, 2 mL pTHF solutions of **1** and **2** were placed into quartz cuvettes (10 mm × 10 mm × 35 mm) and temporal changes in the absorption spectra were measured spectrophotometrically. Whereas a microcuvette (1 mm × 1 mm × 10 mm) was used in the fluorescence method, and the changes in the fluorescence spectra during irradiation were measured with spectrofluorimeter.

The quantum yields of the photodecomposition processes under two-photon excitation, Φ_{2PA}, were determined with the experimental setup presented in Fig. 2b. The values of Φ_{2PA} were obtained by the fluorescence method [17,20], using the PTI spectrofluorimeter and femtosecond laser system described above. Calculations of Φ_{2PA} were performed from the initial slope of the dependencies $F(t)$ [17,20] using a Gaussian spatial and temporal beam profile approximation.

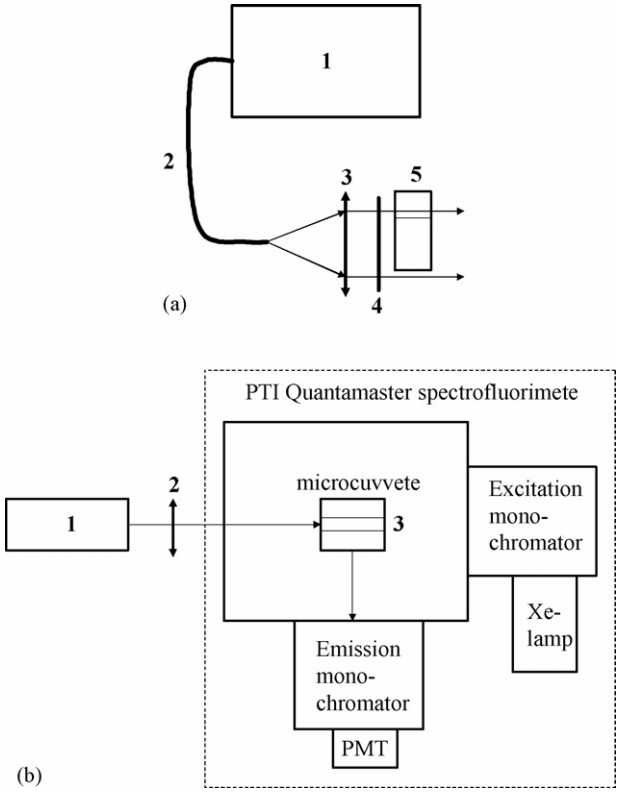

Fig. 2. Schematic diagrams of the experimental setup. (a) One-photon excitation: 1, UV-lamp (LOCTITE 97034); 2, liquid waveguide; 3, lens (5 cm); 4, glass UV–visible filters; 5, 10 mm × 10 mm × 35 mm quartz cuvette. (b) Two-photon excitation: 1, femtosecond laser system (CPA2010); 2, lens (30 cm); 3, 1 mm × 1 mm × 10 mm quartz microcuvette.

Photochemical products of **1** and **2**, formed in pTHF (after one-photon excitation), were analyzed by HPLC and mass spectrometry (MS). A Waters HPLC instrument equipped with a binary pump (1525), an in-line degasser, a PDA detector (2996) and a manual injector (7725I) was used for HPLC analysis. The best chromatographic separation was achieved by using a silica gel analytical column (4.6 mm × 150 mm, particle size 5 μm, pore size 100 Å), with a mobile phase of 97:3 hexane:ethyl acetate in isocratic flow mode. The flow rate was 1.0 mL/min, the injection volume was 50 μL, the column temperature was 30 °C and the run time was 16 min.

Atmospheric pressure chemical ionization mass spectrometry (APCI-MS) was performed with a Thermo-Finnigan LCQ Duo LC-MS instrument equipped with an UV detector (UV6000 PDA), an APCI source (Thermo-Finnigan), and an ion-trap. Samples were analyzed using APCI ionization and monitored in the positive ionization mode (nitrogen was used as both nebulizer and dryer gas). The vaporizer and capillary temperatures were 450 and 200 °C, respectively. The corona discharge voltage (4.5 kV), sheath gas flow (48 a.u.), auxiliary gas flow (3 a.u.), discharge current (10 μA), capillary voltage (38 V), and the SID fragmentor voltage (6 V) were determined by tuning the mass analyzer by infusing a solution of **1** and **2** at 10 μL/min and monitoring the mass-to-charge ratios in the region of 100–1500 u. The injection volume was 100 μL. Data was acquired and processed with the software Xcaliber v1.2.

3. Results and discussion

3.1. Spectral properties

The absorption, fluorescence, and excitation anisotropy spectra of **1** and **2** in pTHF are shown in Fig. 3. The shapes of the fluorescence spectra were independent of the excitation wavelength over the entire spectral range of the measurements. The changes in the excitation anisotropy spectra (curves 3) revealed the spectral position of different electronic transitions in the absorption spectrum. Linear fluorene **1** (Fig. 1) exhibited a fairly constant value of anisotropy in the long wavelength absorption band, corresponding to one electronic transition in this spectral range (370–470 nm). In contrast, a decrease in the anisotropy of branched compound **2** revealed at least two different electronic transitions in the main absorption band (360–480 nm). We recently reported a comprehensive analysis of the electronic structure of **1** and **2**, including quantum-chemical calculations [26]. Extinction coefficients of **1** and **2** for the determination of one-photon photodecomposition quantum yields were obtained in THF, and nearly equal to each other $\varepsilon(\lambda_{max}) \approx 10^5\ M^{-1}\ cm^{-1}$ (λ_{max} is the wavelength of the corresponding maximum).

Two-photon absorption cross-sections, σ_{2PA}, were determined in pTHF at the excitation wavelength, $\lambda_{exc} = 840$ nm, by two different methods (open aperture z-scan [22] and up-converted fluorescence techniques [23] with femtosecond excitation). The values of σ_{2PA} for **1** and **2** were 270 ± 50 GM and 460 ± 80 GM, respectively. Both methods gave similar results for the σ_{2PA}. High fluorescence quantum yields of **1** and **2** (~0.9–1.0) [21], in combination with relatively large σ_{2PA}, make these compounds quite promising for application in 3D fluorescence imaging and optical data storage.

3.2. One-photon photochemical stability

The quantum yields of the photochemical reactions of **1** and **2** in pTHF, Φ_{1PA}, were determined by the absorption and fluorescence methods described above. Kinetic changes in the absorption and fluorescence spectra under UV irradiation are presented in Figs. 4 and 5. The initial slopes of the temporal dependences of the optical density, $D(t)$, and fluorescence intensity, $F(t)$, were used for the quantum yield calculations. The values of Φ_{1PA} obtained by the two different methods are listed in Table 1. Both methods afforded nearly the same photochemical stability results, providing a high degree of self-consistency. Taking into account the large differences in the concentrations for absorption ($C \approx 2 \times 10^{-5}$ M) and fluorescence

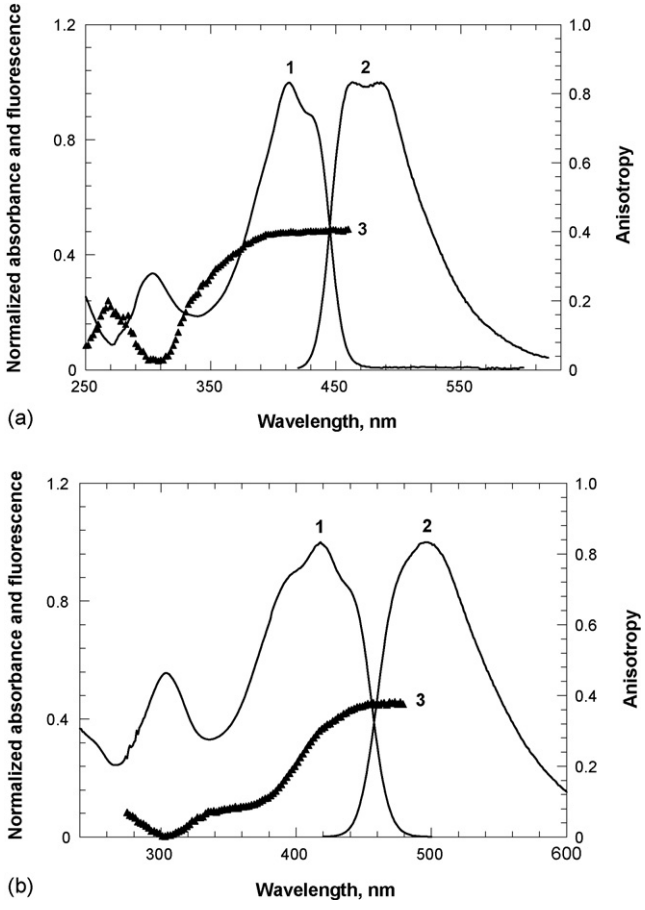

Fig. 3. Absorption (1), corrected fluorescence (2), and excitation anisotropy (3) spectra of (a) **1** and (b) **2** in pTHF. Excitation anisotropy spectra (3) were observed at the emission wavelengths (a) 500 nm and (b) 510 nm, respectively.

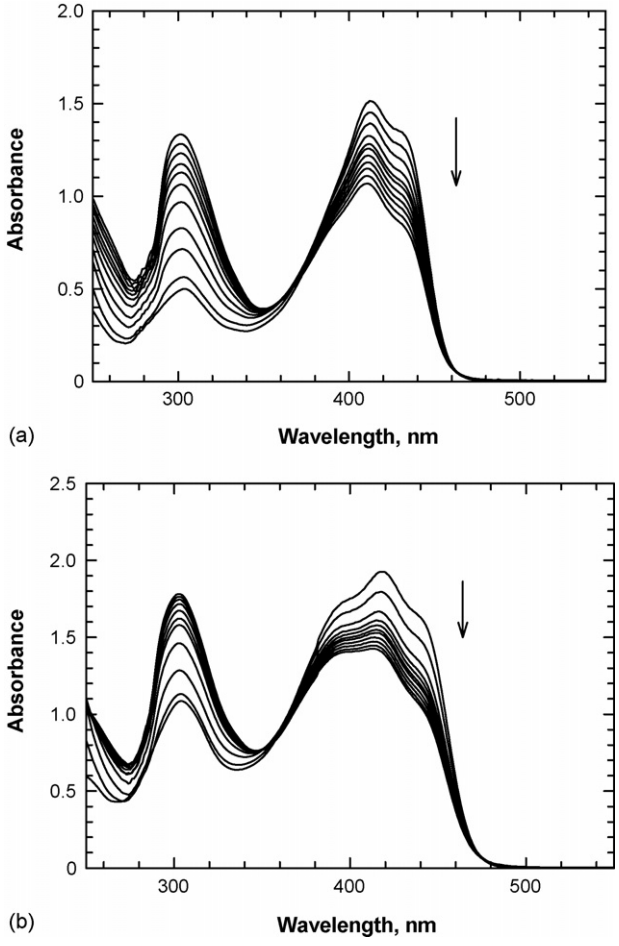

Fig. 4. Kinetic changes in the absorption spectra of (a) **1** and (b) **2** in pTHF upon irradiation at $\lambda_{exc} \approx 420$ nm. The temporal interval between adjacent spectra was 10^3 s. Excitation irradiance, $I_0 \approx 130\ mW/cm^2$.

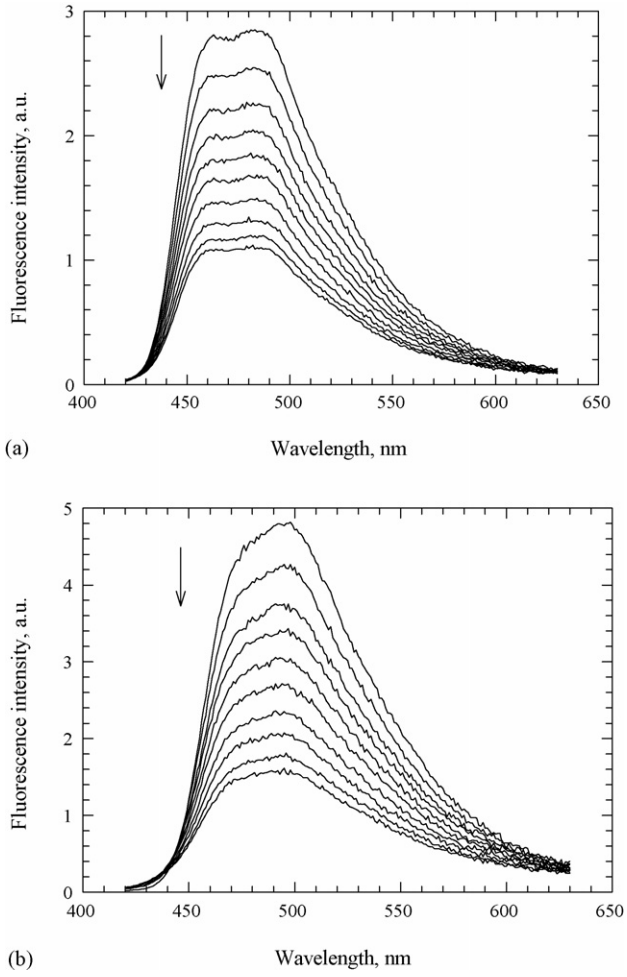

Fig. 5. Kinetic changes in the fluorescence spectra of (a) **1** and (b) **2** in pTHF upon irradiation at $\lambda_{exc} \approx 420$ nm. The temporal interval between adjacent spectra was 360 s. Excitation irradiance, $I_0 \approx 130\,mW/cm^2$.

methods ($C \approx 10^{-6}$ M), one can assume first order photoreaction of **1** and **2** in pTHF (i.e., photodecomposition is independent of concentration). Deoxygenation of pTHF increased the photostability of **1** and **2** under UV irradiation by at least an order of magnitude (Table 1), indicating the important role of molecular oxygen in the photobleaching (photodecomposition) processes. To our knowledge, the values of $\Phi_{1PA} \sim 10^{-7}$ (in deoxygenated solutions) are among the highest level of UV photochemical stabilities reported for large conjugated organic compounds (e.g., the yields of photobleaching of typical coumarin dyes in aqueous solution are in the order of 10^{-3}–10^{-4}, and 7.5×10^{-6} for Rhodamine 6G) [27]. Thus, compounds **1** and **2** possess desirably high photostability, critical for practical applications as optical and photonic materials.

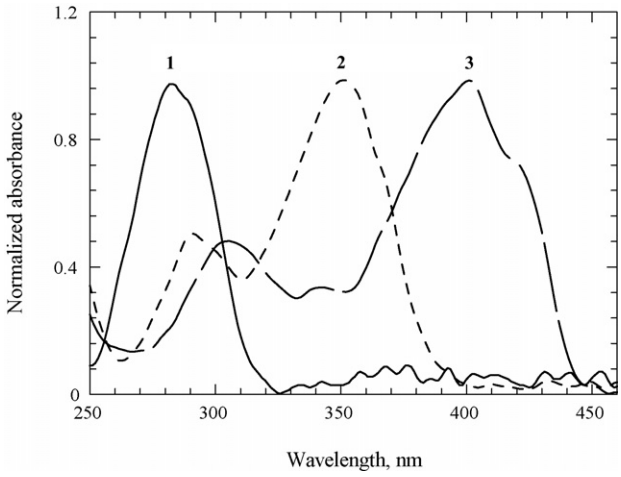

Fig. 6. Absorption spectra of the photoproducts of **1**: (1) **1**Ph3 ($\lambda_{max} \approx 283$ nm), (2) **1**Ph5 (($\lambda_{max} \approx 351$ nm) and (3) **1**Ph6 (($\lambda_{max} \approx 403$ nm).

3.3. Two-photon photochemical stability

The two-photon induced quantum yields, Φ_{2PA}, of the photodecomposition of **1** and **2** (Table 1), were determined by the fluorescence method from the initial slopes of the temporal dependences of the two-photon induced up-converted fluorescence, $F(t)$, shown in Fig. 6. The same values of Φ_{2PA} were obtained for two different concentrations, supporting the predominance of first-order photoreactions. The excitation wavelength, $\lambda_{exc} = 840$ nm, energetically corresponds to the linear UV-lamp irradiation at $\lambda_{exc} \approx 420$ nm. Thus, it is reasonable to assume excitation to the same excited electronic state of **1** and **2** during photoexcitation under UV and fs near-IR irradiation (one- and two-photon excitation, respectively). The corresponding one- and two-photon photodecomposition quantum yields, Φ_{1PA} and Φ_{2PA}, are shown in Table 1. From this comparison, **1** and **2** had nearly the same photodecomposition quantum yields $\sim(1.5–2) \times 10^{-6}$ under one- and two-photon excitation, suggesting similar mechanisms of photodecomposition of **1** and **2**. This high level two-photon photostability of both **1** and **2** is a promising feature of the compounds for a number of non-linear optical and photonic applications.

Table 1
Quantum yields of the photoreactions of **1** and **2**, Φ_{1PA} and Φ_{2PA}, in air-saturated and deoxygenated pTHF under one- and two-photon excitation at 420 and 840 nm, respectively

Compound, solvent condition	Absorption method $\Phi_{1PA} \times 10^6$ [C] (M)	Fluorescence method $\Phi_{1PA} \times 10^6$ [C] (M)	Fluorescence method $\Phi_{2PA} \times 10^6$ [C] (M)
1 Air-saturated	2.0 ± 0.2 [1.8×10^{-5}]	1.9 ± 0.2 [1×10^{-6}]	1.9 ± 0.5 [1.8×10^{-5}, 1×10^{-6}]
1 Deoxygenated	0.12 ± 0.02 [1.8×10^{-5}]	–	–
2 Air-saturated	2.1 ± 0.2 [1.9×10^{-5}]	2.0 ± 0.2 [1×10^{-6}]	1.5 ± 0.4 [1.9×10^{-5}, 1×10^{-6}]
2 Deoxygenated	0.2 ± 0.05 [1.9×10^{-5}]	–	–

C is the concentration of solution in M.

Table 2
Fragment ions in the APCI mass spectra of photoproducts **1**Ph2, **2**Ph2, **2**Ph3 and **2**Ph4

Photoproduct	Fragment ions	Photoproduct	Fragment ions	Photoproduct	Fragment ions
1Ph2	167.22	**2**Ph1	223.14	**2**Ph3	167.24 $[M+H]^+$
	244.28 $[M+H]^+$		251.15		244.30
	245.32		301.17		245.25
	274.16		329.14 $[M+H]^+$		274.24
	294.27		391.19		327.13
	465.70		405.24		437.23
	738.81				767.43
1Ph6	166.15	**2**Ph2	231.23	**2**Ph4	231.20
	256.40		298.29		274.22 $[M+H]^+$
	272.24		383.14 $[M+H]^+$		275.19
	279.36		439.16		579.24
	399.24		495.18		705.40
	475.37 $[M+H]^+$				789.37
	476.36				790.38
	505.36				791.32
	719.44				

$[M+H]^+$ indicates the molecular ion.

3.4. Cursory photoproduct analysis of *1*

In order to understand the type of photodecomposition processes incurred by **1** and **2**, separation and characterization of photoreaction mixtures was undertaken. Normal phase HPLC proved useful for the separation of several photoproducts of **1** and **2**. Photodecomposition of **1** in pTHF under UV irradiation resulted in 6 main photoproducts **1**Ph1–**1**Ph6, with retention times of: **1**Ph1 at 2.1 min, **1**Ph2 at 2.4 min, **1**Ph3 at 3.9 min, **1**Ph4 at 6.9 min, **1**Ph5 at 7.5 min, and **1**Ph6 at 9.0 min. The retention time of unreacted **1** was 4.3 min. Peak purity test for the peaks of **1**Ph1 and **1**Ph2 showed that they did not consist of a single compound, and, therefore, were excluded from analysis. The signal-to-noise ratio of **1**Ph4 was less than 3 and was also excluded from this cursory analysis. The absorption spectra of **1**Ph3, **1**Ph5, and **1**Ph6 (extracted from the PDA detector) are shown in Fig. 6. The spectral shapes of the absorption bands of **1**Ph5 and **1**Ph6 are similar to the structurally related compound 2,7-diphenylamino-9,9-didecylfluorene [24], showing a short wavelength maximum at ≈300 nm.

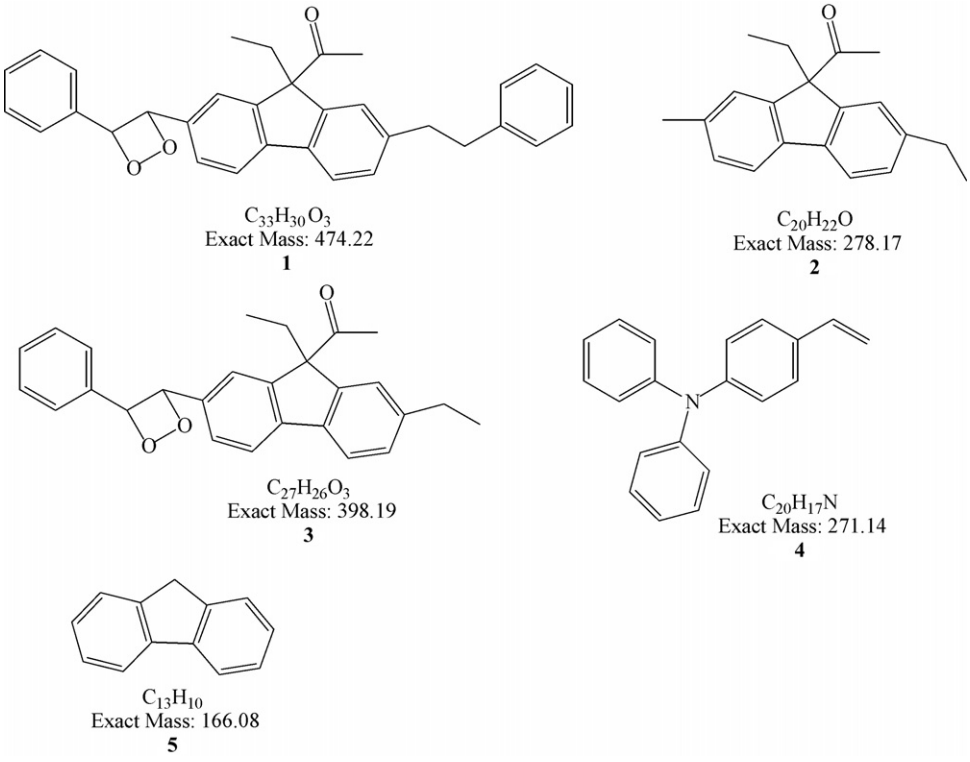

Fig. 7. Possible structures of fragment ions at *m/z* 166.15, 272.24, 279.36, 399.24, and 475.37 in the full scan APCI mass spectrum of **1**Ph6.

In order to better understand the photodegradation process, the APCI mass spectra of **1**, and the most abundant photoproducts (**1**Ph5 and **1**Ph6) were obtained. Mass spectra of other photoproducts (**1**Ph3 and **1**Ph4) could not be detected accurately, since the amounts of these photoproducts formed was too low. Negative ionization mode did not provide useful information. In contrast, positive ionization mode yielded reproducible mass spectral data. Fragment ions and the molecular ion for **1**Ph5 are given in Table 2. Based on the analysis of the APCI mass spectra and Ref. [28], some possible structures of fragment ions of **1**Ph6 are shown in Fig. 7. Since aromatic amines are generally photostable [28], photochemical reactions were expected to involve other functional groups in the molecule, particularly the olefinic C=C double bonds. Some of the proposed fragments can be explained by the [1 + 2] cycloaddition reaction of oxygen with an olefinic C=C double bond of **1**, and by hydrogen abstraction from the alkyl chain with radical formation, subsequent oxidation, and cleavage to produce fragments 1–3, quite reasonably suggesting that oxygen is involved in the mechanism of photodegradation. This is by no means an exhaustive analysis but lends support to the oxygen-dependence of the photochemical decomposition quantum yields described in the previous sections.

3.5. Cursory photoproduct analysis of *2*

Photobleaching of **2** under UV irradiation resulted in four main photoproducts (**2**Ph1–**2**Ph4). The absorption spectra of **2**Ph1–**2**Ph4 of **2** are shown in Fig. 8. The profiles of the absorption bands of **2**Ph3 and **2**Ph4 were similar to the structurally related compound 2,7-diphenylamino-9,9-didecylfluorene (with shorter conjugated length) [24] and also to the parent compounds **1** and **2** (Fig. 3b), respectively. An estimation of the possible reaction pathways was based on the APCI mass spectra of **2**, and **2**Ph1–**2**Ph4, presented in Table 2. Due to the high photostability of **2**, the analysis of photoproducts by HPLC-MS proved difficult, due to the low amount of material available, even after very long irradiation times and high concentrations. Similar to derivative **1**, photochemical reactions were expected to involve

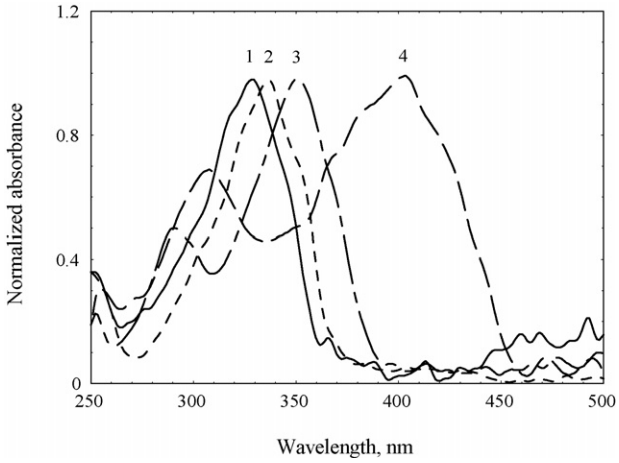

Fig. 8. Absorption spectra of the photoproducts of **2**: (1) **2**Ph1 (λ_{max} ≈329 nm), (2) **2**Ph2 (λ_{max} ≈336 nm), (3) **2**Ph3 (λ_{max} ≈351 nm), and (4) **2**Ph4 (λ_{max} ≈403 nm).

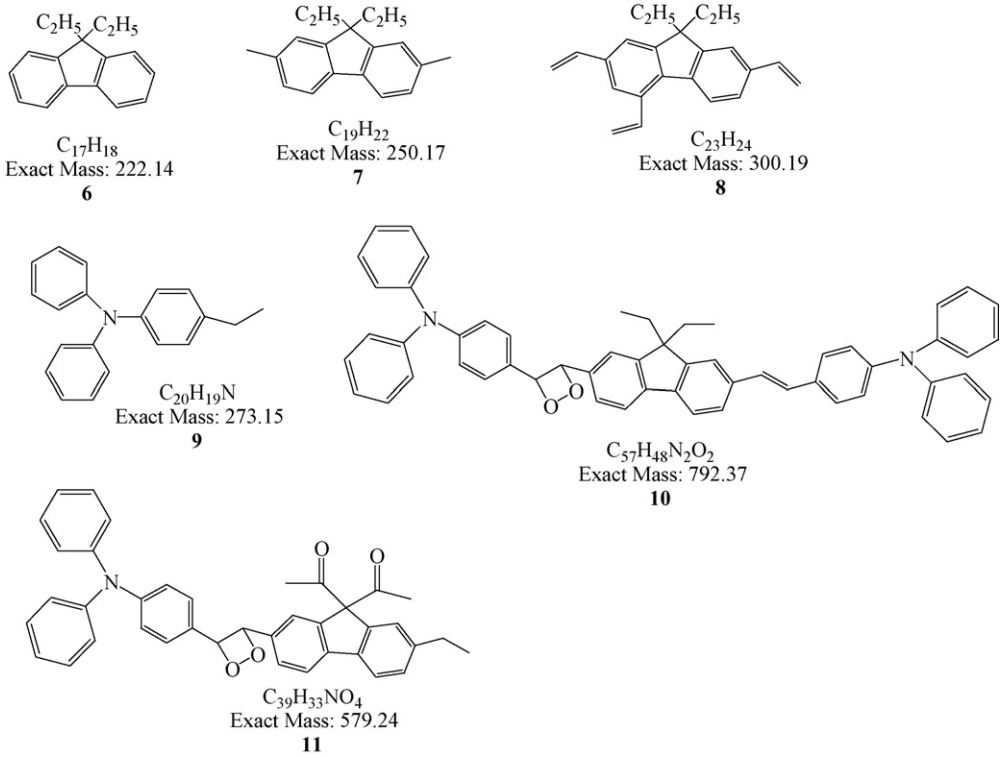

Fig. 9. Possible structures of the fragment ions at *m/z* 223.14, 251.15, and 301.17 in the full scan APCI mass spectrum of **2**Ph1, at *m/z* 274.0 in the full scan APCI mass spectrum of **2**Ph3 and **2**Ph4, and at *m/z* 791.32 and 579.24 in the full scan APCI mass spectrum of **2**Ph4.

other functional groups in the molecule, such as olefinic C=C double bonds.

Based on these assumptions and analysis of Ref. [28], the structures of some possible fragment ions of **2**Ph1 and **2**Ph3 can be proposed (Fig. 9). Molecular oxygen also can participate in the photoreactions resulting in the formation of possible structures (Fig. 9).

In order to determine a possible role of singlet oxygen ($^1O_2$) in the photodecomposition mechanism of **1** and **2**, $^1O_2$ was generated by sensitization of a well known singlet oxygen sensitizer (methylene blue, singlet oxygen quantum yield (Φ_Δ): 0.49) and the photodecomposition products of **2** were compared to the previously detected ones. Primarily **2** and methylene blue were recovered, and no evidence of the presence of previously detected photodecomposition products was found. Results from this experiment, along with the quantum yield data described above, suggest that ground state oxygen, rather than $^1O_2$ is involved in the photodecomposition of **1** and **2**.

4. Conclusions

The one- and two-photon photochemical stability of two promising, non-linear absorbing fluorene derivatives was investigated using both absorption and fluorescence methods under excitation in air-saturated and deoxygenated pTHF. The quantum yields of the photochemical reactions exhibited no concentration dependence, consistent with first-order photodecomposition processes. The values of the photochemical decomposition quantum yields were in the range $\Phi_{1PA} \approx (1.9–2.1) \times 10^{-6}$ and $\Phi_{2PA} \approx (1.5–1.9) \times 10^{-6}$ for one- and two-photon excitation, respectively. Close values of Φ_{1PA} and Φ_{2PA} provide strong support for similar photobleaching processes of **1** and **2** for both types of excitation. In deoxygenated pTHF, the photostability of **1** and **2** increased by at least an order of magnitude relative to that in air-saturated solutions, revealing an important role of molecular oxygen in the photoreactions. Several photochemical products of **1** and **2** were resolved by HPLC and investigated by APCI-MS spectroscopy. The analysis of the mass spectra provides insight into the possible reaction pathways and confirmed participation of the molecular oxygen in photobleaching processes. Results from experiments with a known $^1O_2$ photosensitizer show no additional photoproducts, suggesting that ground state oxygen rather than $^1O_2$ was involved.

Fluorene derivatives **1** and **2**, possess large two-photon absorption cross-sections, high fluorescence quantum yields, and high one- and two-photon photochemical stability, highly desirable attributes for use in a number of emerging linear and non-linear optical applications; particularly for 3D fluorescence imaging and optical data storage, topics to be reported on separately in the future.

Acknowledgments

We wish to acknowledge the U.S. Civilian Research and Development Foundation (UK-C2-2574-MO-04), the donors of The Petroleum Research Fund of the American Chemical Society, the Research Corporation Cottrell College Science program, the National Research Council COBASE award, the Florida Hospital Gala Endowed Program for Oncologic Research, the National Science Foundation (ECS-0217932 and DMR-9975773), and the University of Central Florida Presidential Initiative for Major Research Equipment for partial support of this work.

References

[1] K.D. Belfield, F.E. Hernandez, I. Cohanoschi, M.V. Bondar, E.W. Van Stryland, Polym. Mater.: Sci. Eng. 91 (2004) 346–347.
[2] G.S. He, T.-C. Lin, P.N. Prasad, R. Kannan, R.A. Vaia, L.-S. Tan, J. Phys. Chem., B 106 (2002) 11081–11084.
[3] O. Mongin, L. Porres, C. Katan, T. Pons, J. Mertz, M. Blanchard-Desce, Tetrahedron Lett. 44 (2003) 8121–8125.
[4] I. Wang, P.L. Baldeck, C. Martineau, G. Lemercier, J.-C. Mulatier, C. Andraud, Nonlinear Opt., Quant. Opt. 32 (1–3) (2004) 161–173.
[5] Y. Morel, A. Irimia, P. Najechalski, Y. Kervella, O. Stephan, P.L. Baldeck, C. Andraud, J. Chem. Phys. 114 (2001) 5391–5396.
[6] K.D. Belfield, K.J. Schafer, Y. Liu, J. Liu, X. Ren, E.W. Van Stryland, J. Phys. Org. Chem. 13 (2000) 837–849.
[7] M.P. Ligocki, C. Leuenberger, J.F. Pankow, Atmos. Environ. 19 (1985) 1609–1617.
[8] R.M. Dickhut, K.E. Gustafson, Environ. Sci. Technol. 29 (1995) 1518–1525.
[9] J. Sabate, J.M. Bayona, A.M. Solanas, Chemosphere 44 (2001) 119–124.
[10] L. Moeini-Nombel, S. Matsuzawa, J. Photochem. Photobiol. A: Chem. 119 (1998) 15–23.
[11] J.T. Barbas, M.E. Sigman, R. Arce, R.J. Dabestani, J. Photochem. Photobiol. A: Chem. 109 (1997) 229–236.
[12] J.W. Baur, M.D. Alexander, J.M. Banach, L.R. Denny, B.A. Reinhardt, R.A. Vaia, P.A. Fleitz, S.M. Kirkpatrick, Chem. Mater. 11 (1999) 2899–2906.
[13] J.-D. Guo, Y. Luo, J. Mol. Struct. 635 (2003) 1–9.
[14] F.-J. Kao, Y.-M. Wang, J.-C. Chen, P.-C. Cheng, R.-W. Chen, B.-L. Lin, Opt. Commun. 201 (2002) 85–91.
[15] P.D. Wood, L.J. Johnston, J. Phys. Chem. A 102 (1998) 5585–5591.
[16] P.S. Ditrich, P. Schwille, Appl. Phys. B 73 (2001) 829–837.
[17] K.D. Belfield, M.V. Bondar, O.V. Przhonska, K.J. Schafer, J. Photochem. Photobiol. A: Chem. 162 (2004) 569–574.
[18] K.D. Belfield, S. Yao, J.M. Hales, M.V. Bondar, D.J. Hagan, E.W. Van Stryland, Polym. Mater.: Sci. Eng. 91 (2004) 340–341.
[19] K.D. Belfield, C.C. Corredor, A.R. Morales, M.A. Dessources, F.E. Hernandez, J. Floresc. 16 (2006) 105–110.
[20] K.D. Belfield, M.V. Bondar, O.V. Przhonska, J. Floresc. 16 (2006) 111–117.
[21] S. Yao, K.D. Belfield, J. Org. Chem. 70 (2005) 5126–5132.
[22] M. Sheik-Bahae, A.A. Said, T.H. Wei, D.J. Hagan, E.W. Van Stryland, IEEE Quantum Electron. QE-26 (1990) 760–769.
[23] C. Xu, W.W. Webb, J. Opt. Soc. Am. B 13 (1996) 481–491.
[24] K.D. Belfield, M.V. Bondar, O.V. Przhonska, K.J. Schafer, J. Photochem. Photobiol. A: Chem. 162 (2004) 489–496.
[25] K.D. Belfield, M.V. Bondar, Y. Liu, O.V. Przhonska, J. Phys. Org. Chem. 16 (2003) 69–78.
[26] K.D. Belfield, M.V. Bondar, I. Cohanoschi, F.E. Hernandez, O.D. Kachkovsky, O.V. Przhonska, S. Yao, Appl. Opt. 44 (33) (2005) 7232–7238.
[27] C. Eggeling, L. Brand, C.A.M. Seidel, Bioimaging 5 (1997) 105–115.
[28] Gilbert, J. Bagott, Essentials of Molecular Photochemistry", Blackwell Science Ltd., 1991 (Chapters 6, 9 and 11).